Longitudinal Power Monitoring over a deployed 10,000-km Link for Submarine Systems

Alix May[1], Fabien Boitier[1], Alexis Carbo Meseguer[2], Juan Uriel Esparza[2], Philippe Plantady[2], Alain Calsat[2], and Patricia Layec[1]

[1]Nokia Bell Labs, Route de Villejust, 91620 Nozay, France. [2]Alcatel Submarine Networks Paris-Saclay, 91620 Nozay, France.
alix.may@nokia.com

Abstract: We demonstrate the power profile estimation over a deployed 10,000-km submarine link using digital processing at the receiver. We experimentally show that we estimate span lengths with 0.49km uncertainty and locate multiple power losses. © 2023 The Author(s).

1. Introduction

For the marginless and reliable operation of optical transmissions systems, massive monitoring needs to be deployed to gather as much information as possible about the health and status of the transmission link. To this end, additional hardware is often required, such as the optical time-domain reflectometers (OTDR). This device is not ideal because it requires out-of-band signal. Recent alternatives to estimate the longitudinal power profiles were demonstrated from a single coherent receiver based on nonlinear back-propagation techniques [1] and [2]. Such techniques have been used to demonstrate the monitoring of additional phenomena [3] and have been tested in various conditions, like a meshed optical network [4], or applied to a wavelength-division multiplexed channel [5].

In submarine links, the OTDR is vastly used. However, since transmission involves long distances – sometimes more than 5,000km – averaging time may take hours and even days due to a low signal-to-noise ratio. Longitudinal power profiles techniques are usually demonstrated in links that are less than 400km. For longer links, the amount of added noise makes it more challenging as the method is based on the received signal analysis. In [6], a 2,080-km transmission link – with the use of a recirculating loop – is accurately monitored, which paves the way for longer transmission links. In correlation-based methods [1], [4-5], chromatic pre-dispersion is performed at the transmitter in the order of a third of the total transmission distance, which is impractical in long submarine links.

In this paper, we propose to investigate the longitudinal power monitoring over 10,000km link with a correlation-based method and no chromatic pre-dispersion. We show that we can locate amplifiers and determine span lengths, as well as the possibility to locate power anomalies simultaneously at two positions.

2. System description

The experimental set-up is described in Fig.1. We perform our experiments with a multi-channel transmission with two different spectrum allocations. The channels under test (CUT) are PDM-QPSK modulated at either 32 or 69 Gbaud. They are shaped with a root-raised-cosine filter with 0.01 roll-off factor. Sequences of 2^{17} symbols are used for the transmitted signal. No digital chromatic pre-dispersion is applied. For the transmitted bandwidth, we consider two configurations. For the i) 32-Gbaud case, we consider 1550.12 nm for the CUT. For the ii) 69-Gbaud case, we successively position the CUT at 56 different wavelengths ranging from 1534.25 to 1567.34 nm. The bandwidth is loaded with amplified spontaneous emission (ASE) channels to reach for i) 42 channels 100-GHz spaced or for ii) 56 channels 75-GHz spaced. The channels are sent into a straight line of 56km-long Pure Silica Core Fiber spans with 110 µm² effective area. For the 32-Gbaud case, the line reaches 10,064-km and 10,819-km for the 69 Gbaud case. We amplified the signal using 4.2 THz-wide C-band erbium-doped fiber amplifiers (EDFAs) operated in constant output power mode at 16.5 dBm to approach a real submarine operating point configuration. The input span launch power of each channel is therefore equal to 0.27 dBm in the 32-Gbaud case and -0.98 dBm in the 69-Gbaud case, which is, for the latter, 0.5 dB below the nonlinear threshold. The CUT is then sent to an offline coherent receiver with 70 GHz

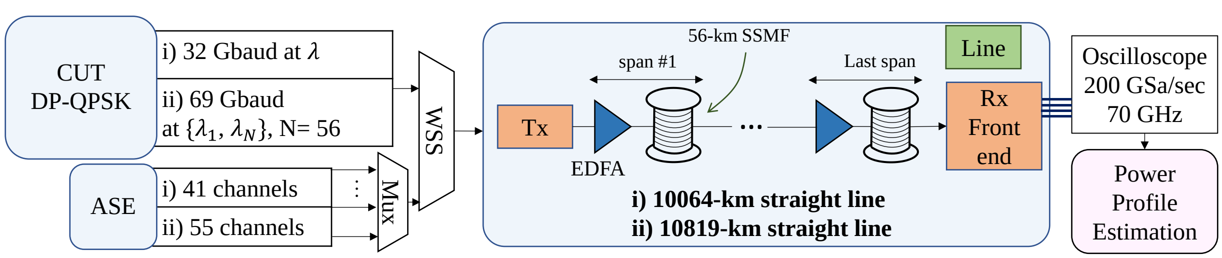

Figure 1: Experimental set-up. WSS: wavelength selective switch. Mux: multiplexer. SSMF: standard single mode fiber.

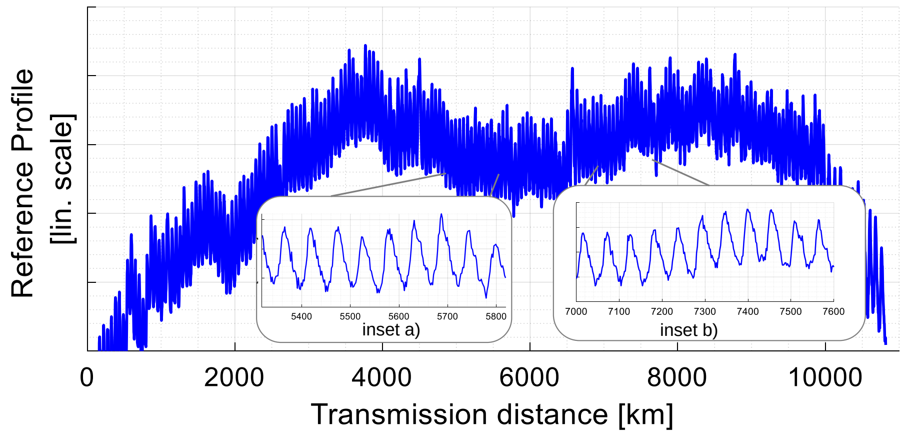

Figure 2: Experimental results. Power profile computed for the whole 10,819-km line at 69 Gbaud. Insets zoom the profile for [5320-5820]km (a) and [7000-7600]km (b)

bandwidth and 200 GSamples/s real-time oscilloscope and process offline. For the (ii) case, we record 2 acquisitions for each of the 56 channel frequencies leading to 112 acquisitions of 2.6×10^6 samples – at 2 samples per symbol (sps). Finally, for the (i) case, to emulate power anomalies, we modify the amplifier gain at the beginning of two spans. We record 100 acquisitions of 1.6×10^6 samples – at 2 sps – in each of the 3 configurations: no attenuation, a 3dB anomaly at 4804 km, two 3dB anomalies at 4804 km and 7111 km.

3. Results and discussion

The power profiles are computed using the algorithm described in [1] from the samples acquired by the oscilloscope. In brief, it computes the correlation between a reference field and the partially non-linearly compensated field. As in [6], we assume the transmitted sequence is known and acts as the reference field. The correlation is done with the fields at 2 sps. To map the distance with the chromatic dispersion, we use the ratio of the accumulated value of the dispersion over the total distance to define the amount of CD to be compensated at each coordinate of the profile. However, this ratio is only an average value and adds uncertainty to the coordinates.

We plot in Fig.2 the power profile for 69 Gbaud through the whole link and in insets the zooms of the same power profile on restricted distance. The step chosen in Fig2a) and Fig. 2b) is 2 km, meaning for example that for the axis 7000-7600 km, 300 coordinates were computed. This profile was computed using the 112 acquisitions. In Fig.2, we see that a curved shape convolutes the profile. This shape is usually flatten by applying a positive chromatic pre-dispersion to the transmitted signal as done in [1], [4-5], where it was of the order of a third of the total transmission distance. However, for long submarine links, it is not realistic as the dispersion will be too large at the transmitter, hence requiring a very long filter to be added. That is why we propose to use a correlation-based method but with no chromatic pre-dispersion. In Fig. 2a) and Fig. 2b), we see that the peaks are distributed periodically, which shows that the spans have the same length. To estimate the accuracy of the measured topology, we calculate, for 22 sets of 5 acquisitions, the distance for 10 spans for Fig.2.b) and then we average. We get a mean value of 54.9 km with a standard deviation of 0.49 km for the average span length over these 10 spans, which is close to the averaged span length of 55.3 km in this distance range. We recall that the step used is 2 km and therefore the maximum accuracy is 0.2 km (i.e., step size/number of spans). To sum up, by leveraging the number of channels to compute power profiles, we can infer the topology of the 10,819-km link, here demonstrated on a subset of the link, fitting well the actual topology.

Finally, we focus on the monitoring of power anomalies. This study is performed on the 32 Gbaud channels acquisitions. In a first step, we compute a reference power profile. We plot this profile in Fig.3a for two distance ranges to ease the visibility. In a second step, we generate one 3-dB anomaly at 4804km, compute a first monitoring power profile, and we generate an additional 3-dB anomaly at 7111km, and compute a second monitoring power profile. We finally compute anomaly indicator (AI), the difference between the reference and the monitoring power profile, in Fig.3b). Each AI and power profile were computed averaging 20 profiles (from 20 acquisitions). Note that the dispersion value used here to map the distance is 20.7 ps/nm/km. We successfully observe one peak when one loss is inserted and two peaks when two losses are inserted. We also see that the peaks are well located. After each peak, the AI returns to a flat floor which indicates that the anomaly was well compensated by the following EDFA. We now study the accuracy on the location of the anomaly. To do that, we estimate the position of both anomalies by measuring the maximum of the derivative of the AI as described in [1]. For each anomaly, we perform multiple estimations. We

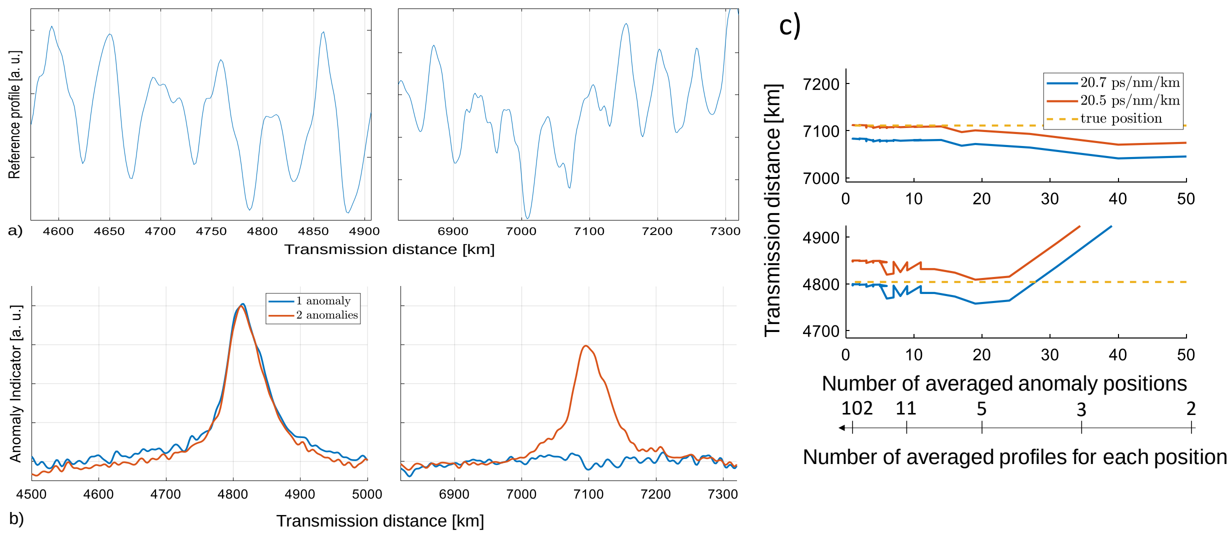

Figure 3: Experimental results. a) Power profile computed at 32 Gbaud for [4500-5050]km and [6850-7350]km. b) Anomaly indicators computed for same x-axis for one 3-dB loss at 4804km and two 3-dB loss at 4804 and 7111km. c) Estimated anomalies using the derivative of the AI when using either 20.5 or 20.7 ps/km/nm.

keep constant the total number of samples used: either we average the 102 power profiles or the found anomaly locations or a mix of both for intermediate cases. We plot in Fig.3c), the mean location estimation for each anomaly as well as their real position.

For the used dispersion of 20.7ps/nm, we observe a good matching for a large number of averaged profiles for the anomaly at 4804km whereas for the second anomaly the mismatch reaches 30km. The estimated location reaches a plateau with more than 5 averaged power profiles. Below that, the estimation error becomes high as the peak is not well defined. To highlight the technique sensitivity to very long distances, we also plot the mean location computed with a different averaged dispersion of 20.5ps/nm. We see that the estimation for the second anomaly is improved while the other is not. A small variation of the dispersion value can lead to an error of 20km. Therefore, to be accurate at each anomaly position, we would need to precisely map the accumulated dispersion at each coordinate. This effect would be negligible in shorter links.

Conclusion

We demonstrate longitudinal power profile monitoring over a deployed link of more than 10,000km thanks to a receiver-based processing. We are able to infer the topology and to monitor two power anomalies occurring simultaneously at 4,804 and 7,111km. We show the importance of using dispersion map knowledge to get an accurate anomaly location. This demonstration confirms the technique validity for troubleshooting in submarine links.

This work was partly funded by EU Horizon 2020 B5G-OPEN Project (grant agreement 101016663).

References

[1] T. Tanimura, S. Yoshida, K. Tajima, S. Oda, and T. Hoshida, ‘Fiber-Longitudinal Anomaly Position Identification Over Multi-Span Transmission Link Out of Receiver-end Signals’, *J. Lightwave Technol.*, vol. 38, no. 9, pp. 2726–2733, 2020, doi: 10.1109/JLT.2020.2984270.

[2] T. Sasai *et al.*, ‘Simultaneous Detection of Anomaly Points and Fiber types in Multi-span Transmission Links Only by Receiver-side Digital Signal Processing’, in *Optical Fiber Communication Conf.*, San Diego, California, 2020, p. Th1F.1. doi: 10.1364/OFC.2020.Th1F.1.

[3] T. Sasai, M. Nakamura, E. Yamazaki, S. Yamamoto, H. Nishizawa, and Y. Kisaka, ‘Digital Backpropagation for Optical Path Monitoring: Loss Profile and Passband Narrowing Estimation’, in *2020 European Conference on Optical Communications (ECOC)*, Brussels, Belgium, Dec. 2020, pp. 1–4. doi: 10.1109/ECOC48923.2020.9333191.

[4] A. May, F. Boitier, A. Courilleau, B. Al Ayoubi, and P. Layec, ‘Demonstration of Enhanced Power Losses Characterization in Optical Networks’, in *Optical Fiber Communication Conference (OFC) 2022*, San Diego, California, 2022, p. Th1C.6. doi: 10.1364/OFC.2022.Th1C.6.

[5] M. Sena *et al.*, ‘DSP-Based Link Tomography for Amplifier Gain Estimation and Anomaly Detection in C+L-Band Systems’, *J. Lightwave Technol.*, vol. 40, no. 11, pp. 3395–3405, Jun. 2022, doi: 10.1109/JLT.2022.3160101.

[6] T. Sasai, M. Nakamura, E. Yamazaki, and Y. Kisaka, ‘Precise Longitudinal Power Monitoring over 2,080 km Enabled by Step Size Selection of Split Step Fourier Method’, in *Optical Fiber Communication Conference (OFC) 2022*, San Diego, California, 2022, p. Th1C.4. doi: 10.1364/OFC.2022.Th1C.4.